

Orthopedic surgery planning based on the integration of reverse engineering and rapid prototyping

Dong-Gyu Ahn^{*}, Jun-Young Lee^{**}, Dong-Yol Yang^{***}

^{*} Dept. of Mechanical Eng., Chosun Univ., 375 Seosuk-dong, Gwang-ju 507, Korea

^{**} Dept. of orthopedics, Chosun Univ., 375 Seosuk-dong, Gwang-ju 507, Korea

^{***} Dept. of Mechanical Eng., KAIST, 375-1 Science Town, Daejeon, Korea

Reviewed, accepted August 30, 2004

Abstract

This paper describes orthopedic surgical planning based on the integration of RE and RP. Using symmetrical characteristics of the human body, CAD data of the original bone without damages for the injured extent are generated from a mirror transformation of undamaged bone data for the uninjured extent. The physical model before the injury is manufactured from RP apparatus. Surgical planning, such as the selection of the proper implant, pre-forming of the implant, decision of fixation positions and incision sizes, etc., is determined by a physical simulation using the physical model. In order to examine the applicability and efficiency of surgical planning technology for orthopedics, various case studies, such as a proximal tibia plateau fracture, a distal tibia comminuted fracture and an iliac wing fracture of pelvis, are carried out. As a result of the examination, it has been shown that the orthopedic surgical planning based on the integration of RE and RP is an efficient surgical tool.

Introduction

Rapid prototyping (RP) technology has a potential of rapid manufacturing for three-dimensional parts with a geometrical complexity from a CAD model in the CAD/CAM environment. The application of RP technology has been extended to various fields such as engineering, manufacturing, medical science, education, industrial design and others [1]. Reverse engineering (RE) can directly generate CAD data from the actual object by measuring surfaces of the object through both contact and non-contact methods. In addition, the RE can easily evaluate the accuracy and the geometrical characteristics of the fabricated parts [2]. The integration of RP and RE has

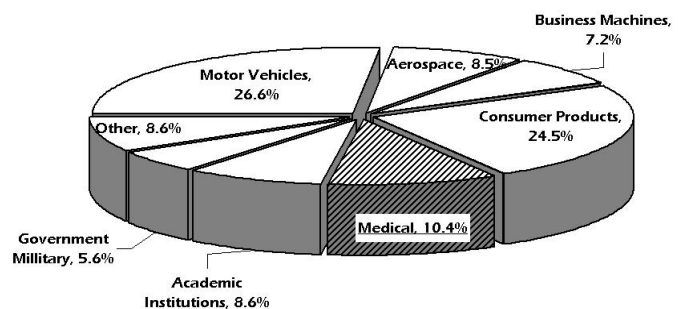


Figure 1: Application area of rapid prototyping [2]

advantages of a rapid duplication for the real things without the risk of damaging the object being duplicated. Bio-medical engineering is one of an application area that utilizes the advantages of the integration of RE and RP. Bio-medical applications have taken 10 % of the market for RP, as shown in Figure 1 [2].

In recent bio-medical engineering, new surgical technologies have been developed to improve the efficiency of surgery, such as the surgical time and the accuracy of surgery, reduce patients' pain and to reduce inaccurate or incomplete surgical treatments [3]. RAS (Robot-assisted surgery) and CAS (Computer-assisted surgery) are representative research areas related to the new orthopedic surgical technologies [4]. Surgical technology based on the integration of RP and RE using CT data has been introduced as an alternative of the CAS.

One of the first researches on the integration of RP and RE using CT data for surgical planning was a cleft palate reconstruction in 1992 [5]. The researches are focused on the manufacture of a physical model for an abnormal face with deformity or damages, and a surgical planning and a prosthesis utilizing the physical model [6]. Recently, the integrated technology has been applied to the field of orthopedic surgery. Potamianos et al. used SLA prototypes to visualize the fractured pelvis and to optimally fix an implant on the skull [7]. Sangheara et al. preliminarily studied the feasibility of applying the integrated technology to medical fields using FDM prototypes [8]. Brown et al. reported the successful in hospital application of RP models in the surgical treatment for the case of the acetabular fractures, insertion pedicle screws in the spine, and long-bone and joint fractures [9]. They employed the reversed CAD data of the intact bone, which is the opposite data to the fractured region, and the Acquta 2100 and Z-CORP machines.

In this paper, an orthopedic surgical planning based on the integration of RE and RP is introduced to improve the efficiency of the orthopedic surgery on bones with symmetrical characteristics. In order to examine the applicability and efficiency of the technology for the surgical planning, various case studies, such as a proximal tibia plateau fracture, a distal tibia comminuted fracture and an iliac wing fracture of pelvis, are carried out. As a result of the examination, it has been shown that the orthopedic surgical planning based on the integration of RE and RP is an efficient surgical tool.

Orthopedic surgery planning based on the integration of RE and RP

The procedure of the orthopedic surgical planning is illustrated in Figure 2. Surgical planning utilizes the symmetrical characteristics of the human body. Computer Tomography (CT) simultaneously scans the injured and uninjured extent of a patient. It verifies the symmetry of the fractured bone using the CT data. The surface reconstruction is performed by

using the CT data. The first .stl data set are subsequently generated from the reconstructed surface. Parts to be considered are selected. In case the target bone is one body, .stl data of both extents, which are the injured and uninjured extents, are generated and the injured extent is removed. The final CAD data of the original bone without damages for the injured extent are generated from the mirror transformation of the intact bone data for uninjured extents, which is an opposite extent to the injured area, as Brown et al. [9] Figure 3 shows the process flow to generate .stl data the original shape for the injured extent. The optimal manufacturing data are generated by the CAD/CAM software of each rapid prototyping machine as steps: determination of building direction, slicing of the .stl data, generation of supports, and in-plane path generation. The physical model of the intact is manufactured from the rapid prototyping machine. The pre-operative surgical planning is decided by the physical simulation using the physical model according to the following steps, as shown in Figure 4: (a) selection of a proper implant, (b) pre-forming of implants, (c) selection of fixation positions, (d) decision of invasive sizes, (e) decision of an approach route for implants, and (e) decision of an approach route of fixing devices for the implants. Finally, the surgical planning and the physical model are used to educate the operators.

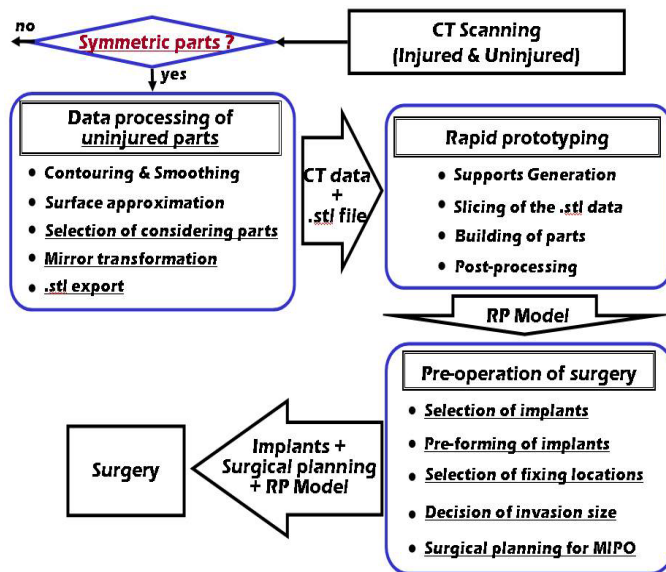


Figure 2: Procedure of the surgical planning based on the integration of RP and RE

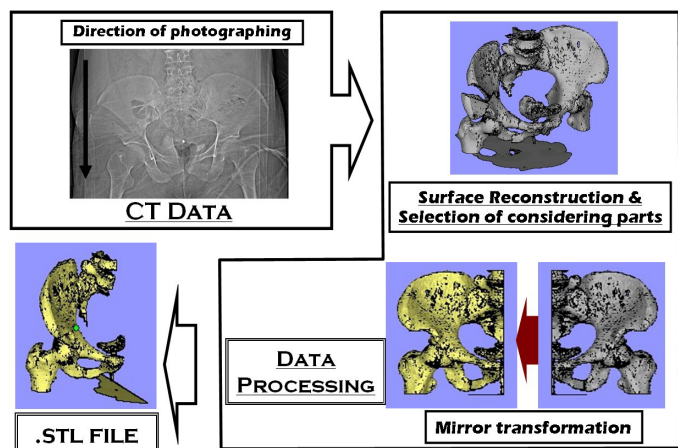


Figure 3: Process flow to generate .stl data of the original shape for the injured extent.

Experiments

Several case studies, such as a proximal tibia plateau fracture, a distal tibia comminuted fracture and an iliac wing fracture of pelvis, are carried out to investigate the applicability and the efficiency of the pre-operative surgical planning technology based on the integration of RP

and RE.

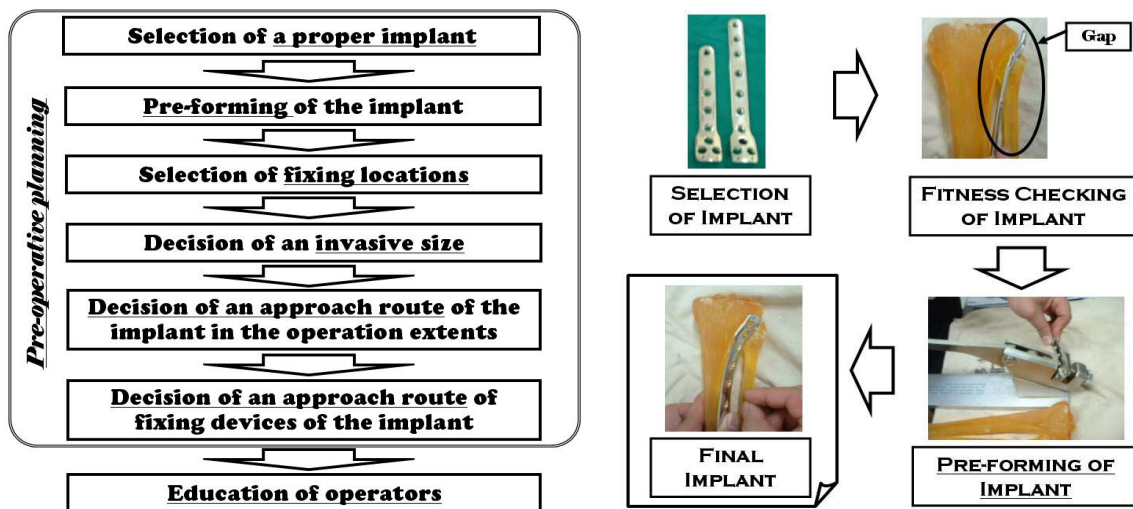


Figure 4: (a) Procedure of pre-operative planning using the physical shape of the original bone shape for injured extents. (b) Pre-operative surgical planning (Selection and pre-forming of implant)

CT data are generated by the SIEMENS SOMATOM Plus 4 scanner. Table 1 shows the slicing interval and a feeding interval of the CT scanner. The CT data are stored in DICOM format.

Table 1: Slicing and feeding interval of CT scanner

Case	Slicing Interval (mm)	Feeding Interval (mm)
Distal tibia comminuted fracture	2.0	1.5
Proximal tibia plateau fracture	2.0	1.5
Iliac wing fracture of pelvis	3.0	2.0

The shape reconstruction of the CT data is performed by MIMICS 6.0 [10]. The direction of the bone shape is identified by the CT data for each direction. Subsequently, the first .stl data are generated from the CT data. Editing of the first .stl data, deleting of the injured extent and generation of a final CAD data through the mirror transformation of the undeleted data are carried out by Magic RP software.

The physical model is manufactured from the Objet Quadra of Objet Inc. [11]. In Objet process, 1530 nozzles selectively shoot the photopolymer on the previous layer in accordance with CAD data, and a UV beam subsequently cures the whole area with the shot photopolymer. These processes are repeated to the final layer. Through this process, a three-dimensional part is rapidly built. The layer thickness of the Objet process is 0.02 mm.

In order to verify the dimensional accuracy of the physical model, an error map is generated by comparing the final CAD data with the measured data of the physical model. The SNX-2W SG non-contact measurement system, which employs a white light and a halogen lamp as the light source and a phase shift/gray code technique, is used to measure the physical model.

Using the physical model, the surgical planning and education of operators are accomplished. The surgery is carried out by the Department of Orthopedics in hospital of Chosun University. The results of surgery are compared with those of the department without utilizing the surgical planning from the viewpoint of the surgical time, the number of X-ray exposures, the invasive size, and patient rehabilitation.

Results and Discussions

Case 1 : Distal tibia comminuted fracture

In this case, a distal tibia of the left foot is fractured. The procedure from generation of CT data to the fabrication of the rapid prototyping model is illustrated in Figure 5. The symmetry of the injured and uninjured extents is obvious, so that a distal tibia of the right foot is scanned by the CT scanner. The original .stl data before injuring are reconstructed by the MIMICS and MagicRP software. The .stl data are generated within ten minutes. The physical model is manufactured from Objet Quadra apparatus using the original .stl data of the injured extents. The error map of the distal tibia shows that the average error is within 0.12 mm, as shown in Figure 6. The results show that the physical model has a good geometrical conformity to the original .stl data. Figure 7 shows the procedure of pre-operative planning and operation of MIPO

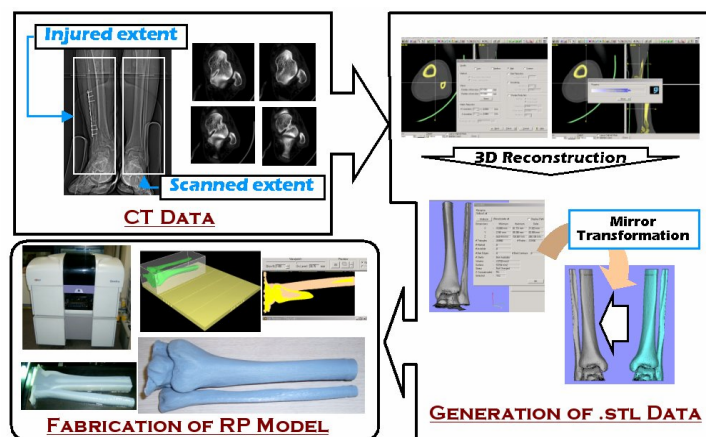


Figure 5: Procedure from CT data to the fabrication of rapid prototyping model of a distal

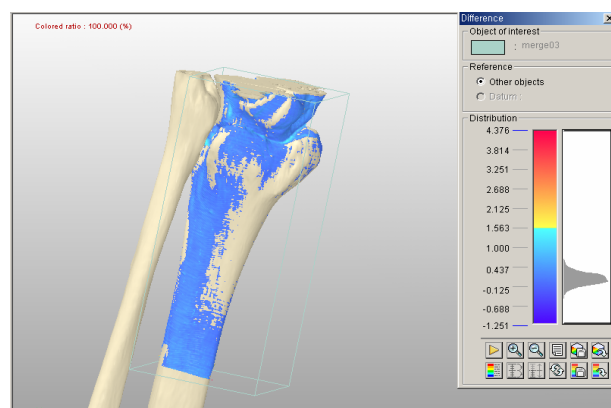


Figure 6: Error map of the physical model for the case of a distal tibia

(Minimal Invasive Percutaneous Plate Osteosynthesis).

Using the physical model, the proper implant is chosen. In addition, the geometry conformity of the implant to the contour of the bone model is verified. Although the implant is an anatomical plate reflected in statistical data of the human body, the results show that the maximum difference between the selected implant and the physical model is 5 mm, as shown in Figure 7. This is because the statistical data of the Korean physique are not reflected in the design data of the implant. Hence, the selected implant is preformed to obtain a good geometrical conformity of the implant to the contour of the physical model. Fixing locations of the implant are selected, as shown in Figure 7. The incision area and the invasive size are selected as “A” in Figure 7 and 2 cm, respectively. In addition, the penetration direction of the implant and the surgical procedure are confirmed.

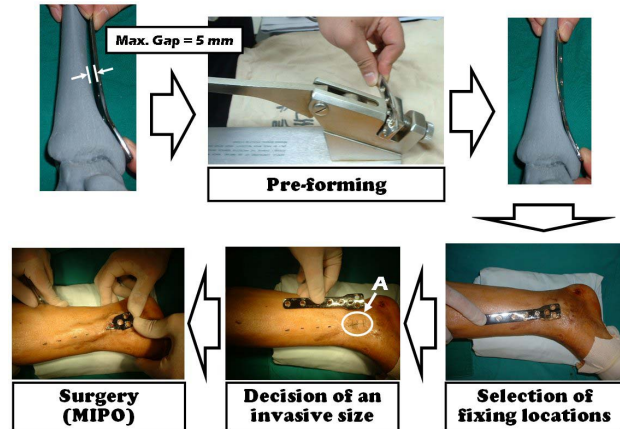


Figure 7: Procedure of pre-operative planning and operation of MIPO for the case of a distal tibia

Table 2: Results of experiment for the case of a distal tibia comminuted fracture

Generation time of .stl data (min)	Size of .stl data (MB)	Building interval (mm)	Avg. error of the physical model (mm)	Surgery Time (min)	# of X-RAY exposures	Invasive Size (mm)
10	12	0.02	0.12	40 (50% Reduction)	1 (70% Reduction)	2 (50% Reduction)

Table 2 and Figure 8 show the results of experiments for the case of a distal tibia comminuted fracture. The results of surgery show that the surgery time, number of X-RAY exposures and the invasive size are forty minutes, one time and 2 cm, respectively. Comparing the results of surgery utilizing the described technology of orthopedic surgery planning with those of a surgery without utilizing the proposed surgical planning in which is conventional surgery technology of the Orthopedics Department in the hospital of Chosun University, the surgery time, number of X-RAY exposures and the invasive size are reduced by fifty percent, seventy



Figure 8: Results of surgery for the case of a distal tibia

percent and fifty percent, respectively. An amount of radiation projected into the patient is decreased due to the reduction of number of X-RAY exposure to identify position of the implant and the invasive size is reduced, so that it is ascribed that the morbidity of patients is highly reduced as well. MIPO has been available because of the reduction of invasive sizes. The residual stress in bone induced by a spring back of implant and splitting between bone and flesh are minimized due to a good geometrical conformity of the preformed implant to the fractured extents of patient, so that the speed of rehabilitation is remarkably enhanced.

Case 2 : Proximal tibia plateau fracture

In this case, a proximal tibia of the left foot is sunken. Because the injured extent is a joint connected to three bones, a three-dimensional physical model of the original bone shape is necessary to establish an accurate surgical planning. The whole procedure from CT data to MIPO is illustrated in Figure 9. Table 3 shows the results of experiment.

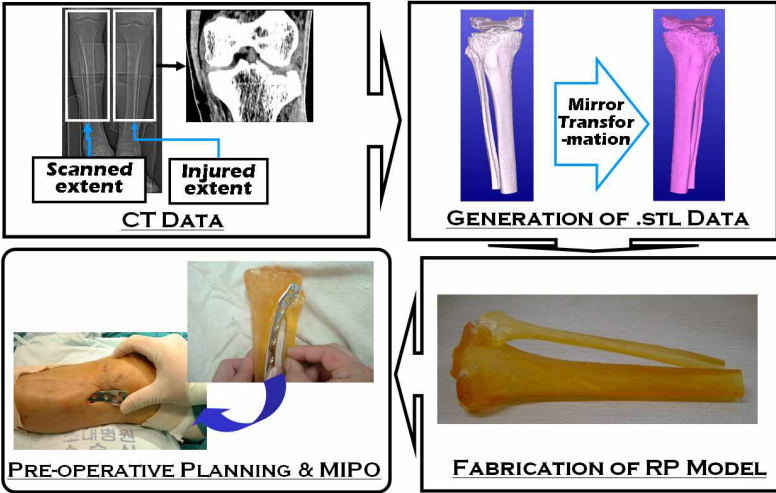


Figure 9: Whole process for the case of the proximal tibia

Table 3: Results of experiment for the case of a proximal tibia plateau fracture

Generation time of .stl data (min)	Size of .stl data (MB)	Building interval (mm)	Avg. error of the physical model (mm)	Surgery Time (min)	# of X-RAY exposures	Invasive Size (mm)
20	7.9	0.02	0.15	40 (50% Reduction)	2 (50% Reduction)	4 (30% Reduction)

The original bone data is generated by the mirror transformation of .stl data for the uninjured extent, as shown in Figure 9. The original .stl data is generated within twenty minutes. The physical model with the uninjured bone shape of the proximal tibia is manufactured from Objet Quadra. The average error of the physical model is less than 0.15 mm. Using the physical model, the proper implant is chosen, and the geometrical conformity of the implant to the uninjured bone shape is verified. From the results of the verification, it is found that the maximum gap between the physical model and the selected implant is 6 mm in the vicinity of knee sides. In addition, it is known that the selected implant requires a bending process to compensate for the gap and fifteen degrees of the twisting to obtain a good

geometrical conformity to the physical model. Fixation locations of the implant, the position of incision and the incision size are selected using the preformed implant and the physical model. In addition, the establishment of the surgical planning for MIPO and the education of operators are performed by using the preformed implant and the physical model. The lower part of the knee is chosen as the position of the incision, and the incision size is selected as 4 cm. In addition, the education of operators is performed.

The results of surgery show that the surgery time, the number of X-RAY exposures and an invasive size are forty minutes, two times and 4 cm, respectively. Comparing the results of surgery utilizing the described technology of orthopedic surgery planning with those of a surgery without utilizing the proposed surgical planning in which is conventional surgery technology of the Orthopedics Department in the hospital of Chosun University, the surgery time, the number of X-RAY exposures and the invasive size are reduced by fifty percent, fifty percent and thirty percent, respectively.

Case 3 : Iliac wing fracture of pelvis

Table 4, Figures 10 and 11 shows the results of experiment for the case of an iliac wing fracture of pelvis.

Table 4: Results of experiment for the case of an iliac wing fracture of pelvis

Generation time of .stl data (min)	Size of .stl data (MB)	Building interval (mm)	Avg. error of the physical model (mm)	Surgery Time (min)	# of X-RAY exposures
15	6.4	0.02	0.33	45 (50% Reduction)	2 (50% Reduction)

CT scans the whole region of pelvis, and the first .stl data with the injured and uninjured extent are generated by MIMICS software. The symmetry of the pelvis is obvious, so that the .stl data of the injured extent are removed. The final .stl data is obtained from the mirror transformation of the .stl data of the uninjured extent in MagicRP software. The final .stl data is generated within fifteen minutes. The physical model without damages is manufactured from Objet Quadra. The error map shows that the average error maintains 0.33 mm, as shown in Figure 10. The error of the

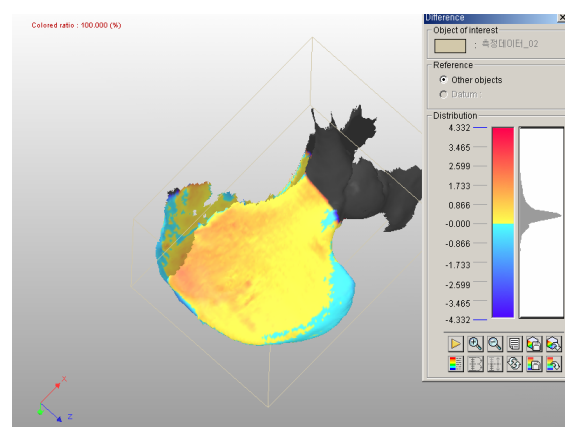


Figure 10: Error map of the physical model for the case of a pelvis

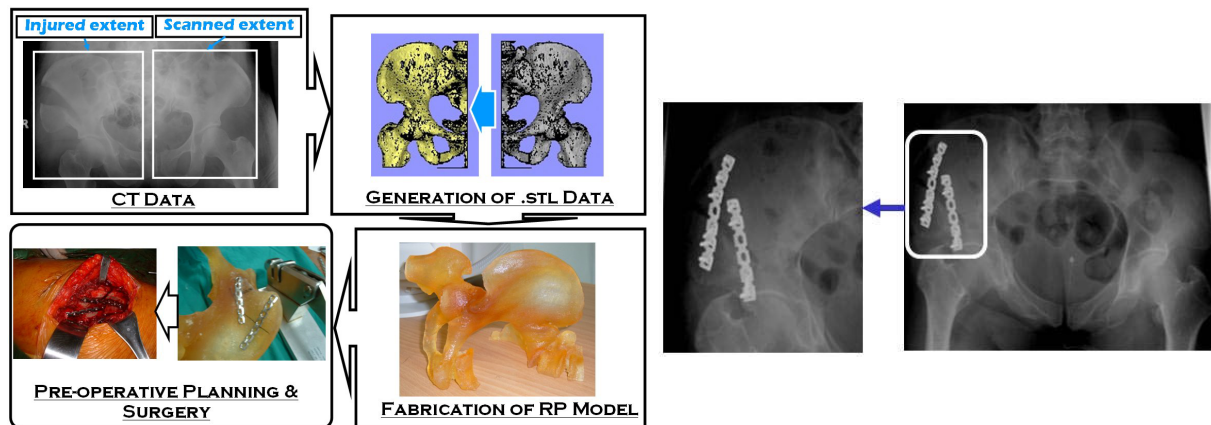


Figure 11: (a) Whole process for the case of an iliac wing fracture of pelvis. (b) Results of experiment

region for wing is, however, less than 0.2 mm. Hence, it has been known that the physical model of the pelvis has a good geometrical conformity to the final .stl data in the region of wing.

Using the physical model, a proper implant is chosen, and the geometrical conformity of the implant to the uninjured bone shape is verified. Because the iliac wing of pelvis has an excessive flexion on the surface of the bone shape, the selected implant should easily bend in conformity with the bone shape. Hence, the pelvic reconstruction plate is chosen as the proper implant. Two pelvic reconstruction plates are needed to accurately fix the fractured extent due to the geometrical characteristics of the iliac wing of pelvis. Fixation locations of the implants, the position of incision and the incision size are chosen using the preformed implants and the physical model. In addition, the establishment of the surgical planning and the education of operators are carried out using the physical model and the preformed implants.

The results of the surgery show that the surgery time and number of X-RAY exposures are forty-five minutes and two times, respectively. Comparing the results of surgery utilizing the described technology of orthopedic surgery planning with those of a surgery without utilizing the proposed surgical planning in which is conventional surgery technology of the Orthopedics Department in the hospital of Chosun University, the surgery time and the number of X-RAY exposures are reduced by fifty percent. An amount of radiation projected into the patient is decreased due to the reduction of number of X-RAY exposure to identify position of the implant. The surgery is successfully carried out without reworking of the implant, which is induced by the difference between the contour of the preformed implant and the bone shape of the patient, in the operating room. The residual stress in bone induced by a spring back of implant and splitting between bone and flesh are minimized due to a good geometrical conformity of the preformed implants to the fractured extent of patient, so that the speed of rehabilitation is remarkably enhanced.

In this case, the fabrication time of the physical model is twenty-six hours. The surgery of the patient is, however, scheduled for one week later after the CT scan. Besides, the fabrication time of the physical model does not affect the surgery schedule. In addition, it has been found that the advantage of the physical modeling in which the rehabilitation speed of the patient is remarkably enhanced by an accurate surgery are greater than the disadvantages of the physical modeling in which an additional cost and a surgical planning time induced by the physical modeling is required.

Conclusions

In this research works, the technology of orthopedic surgical planning based on the integration of RE and RP has been described to apply to the case of bones with symmetrical characteristics. In this technology, the original bone data without damages for the injured extent have been generated from the mirror transformation of the intact bone data for the uninjured extent in which is an opposite extent to the injured area. The physical model has been manufactured from the original bone data. Pre-operative surgical planning, such as the selection of the proper implant, pre-forming of implants, the selection of fixation locations, the decision of invasive sizes, the decision of an approach route for implants, and etc., has been decided by the physical simulation using the physical model. Finally, the education of operators has been carried out utilizing the surgical planning and the physical model. Through the above procedure of the technology for orthopedic surgery planning, the efficiency and accuracy of the orthopedic surgery could be improved.

The applicability and efficiency of the surgical planning technology are demonstrated by various clinical case studies including a proximal tibia plateau fracture, a distal tibia comminuted fracture and an iliac wing fracture of pelvis. The results have been shown that establishment of a desirable surgical planning and the selection of the proper surgical technology are available in the pre-operative planning stage. From the results of the case studies, it has been shown that the surgical time, number of the X-RAY exposures and the invasive sizes are remarkably reduced due to a good geometrical conformity of implants to the bone shape, the fully understanding of geometrical characteristics of bones for the patient and the surgical planning the operators. In addition, it has been found that speed of rehabilitation is remarkably enhanced due to the minimization of the residual stress in bone induced by a spring back of implant and splitting between bone and flesh. Through the reduction of number of the X-RAY exposures and the invasive size, it has been ascribed that the morbidity of patients is highly decreased. Based on the above results, it has been shown that the orthopedic surgical planning based on the integration of RE and RP is an efficient surgical tool.

In the future, additional case studies, such as the complex bones with a serious damage, the bone deficiency with a congenital deformity, and others, Also, an additional statistical evaluations in term of mechanical engineering and medical science should be performed to confirm the applicability of the technology of surgical planning. In addition, the research on the selection of a proper rapid prototyping process, which can overcome the disadvantages of high costs and a long building time to fabricate RP model, should be carried out.

References

1. P. Kulkarni, D. Marson, and D. Dutta, "A Review of Process Planning Techniques in Layered Manufacturing," *Rapid Prototyping Journal*, **6**[1], pp 18-35 (2000)
2. T. Wohler, "Wholer's Report 2003; Rapid Prototyping & Tooling State of the Industry," Wholer's Associates Inc., (2003)
3. W. Sun and P. Lal, "Recent Development on computer aided tissues engineering – a review," *Computer Methods and Programs in Biomedicine*, **67**, pp 85-103 (2002)
4. C. C. Kai, C. S. Meng, L. S. Ching, E. K. Hoe, and L. K. Fah, "Rapid Prototyping Assisted Surgery Planning," *The International Journal of Advanced Manufacturing Technology*, **14**, pp 624-630 (1998)
5. N. G. Stocker, N. J. Mankovitch, and D. Valentino, "Stereolithographic Models for Surgical Planning: Preliminary Report," *Journal of Oral & Maxillofacial Surgery*, **50**, pp 446-471 (1992)
6. P. A. Web, "A Review of Rapid Prototyping (RP) Techniques in the Medical and Biomedical Sector," *Journal of Medical Engineering & Technology*, **24**, pp 149-153 (2000)
7. P. Potamianos, A. A. Aims, A. J. Forester, M. McGurk, and M. Bircher, "Rapid Prototyping for orthopedic surgery," *Proceedings of the Institute Mechanical Engineering Part H : Journal of Engineering in Medicine*, **212**, pp 383-393 (1998)
8. B. Sanghera, S. Naique, Y. Papaharilaou, and A. Amis, "Preliminary study of rapid prototypes medical models," *Rapid Prototyping Journal*, **7**[5], pp 275-284 (2001)
9. G. A. Brown, K. Firoozabkhsh, T. A. Decoster, J. R. Reyna, and M. Moneim, "Rapid Prototyping : The Future of Trauma Surgery ?," *The Journal of Bone and Joint Surgery*, **85-A**[Supplement 4], pp 49-55 (2003)
10. <http://www.materialise.com>
11. <http://www.sysopt.co.kr>